Electronic Supplementary Material (ESI) for Lab on a Chip.

Supplementary Material for

Automatic flow delay through passive wax valves for paper-based analytical devices

Haixu Meng [a], Chang Chen [a,b], Yonggang Zhu [a], Zhengtu Li [c], Feng Ye [c], Joshua Ho [d] and Huaying Chen[a]*

[a] School of Mechanical Engineering and Automation, Harbin Institute of Technology, Shenzhen, Shenzhen 518055, China.

[b] Laboratory of Physical Chemistry and Soft Matter, Wageningen University & Research, Stippeneng 4, 6708 WE Wageningen, the Netherlands.

[c] State Key Laboratory of Respiratory Disease, National Clinical Research Center for Respiratory Disease, The First Affiliated Hospital of Guangzhou Medical University, Guangzhou, China

[d] School of Biomedical Sciences, Li Ka Shing Faculty of Medicine, The University of Hong Kong, Hong Kong, China

* Corresponding Author: chenhuaying@hit.edu.cn, Tel: +86 755 8615 3249

1. Introduction

Table S 1 A list of flow-delay techniques in paper microfluidics

Valve opening method	Delay mechanism	Delay range	Limitations	Application	Reference
Surfactant flows from downstream of the hydrophobic valve	A hydrophobic valve and a delay channel before the valve	Dependent on the length of the delay channel	Sample waste in the delay channel.	ELISA	Lab Chip, 2012,12, 2909-2913
A bridging channel in the bottom layer was employed	The length of the bridging channel	Dependent on the length of the bridging channel	Sample waste in the bridging channel.	ELISA	Lab Chip, 2014, 14, 4042-4049
Surfactant flows through the wax valve	Flow length in the valve and surfactant concentration	about 1-11 minutes	The surfactant needs to be mixed with the sample.	Human IgG detection	Biosensors and Bioelectronics, 2020, 168, 112559
Pre-dried surfactant was dissolved in the sample to flow through wax valves	Surfactant diffusion	a few seconds to around 4 minutes	The Delay mechanism was not well studied.	ELISA	Micromachines, 2019, 10, 837.
Fluid flow vertically through the wax valve by hydrostatic pressure	Wax density in paper and layers of wax-coated paper	30 seconds to 2 hours	Multiple layers introduce fabrication complexity.	Fluid flow control	Analytical chemistry, 2010, 82, 4181-4187
Melting of the wax valve	Manual control through a phase change	Any time period	Requires additional equipment; Complicated to fabricate	Fluid dosing	Lab on a Chip, 2016, 16, 3969-3976
Dissolving of the wax valve using organic solvents	Manual control of the dissolving	Any time period	Requires manual addition of the reagents	Glucose detection	Analytical Chemistry, 2019, 91, 5169-5175.
Surfactant pre-dried a certain distance away from the wax valve	Surfactant diffusion	about 3.6 to 20 minutes	N/A	Detection of glucose or ethanol. Sequential mixing.	---

2. Methods

1.1. Boundary condition

The parameters used in this study were summarized in Table S1.

Table S2 The parameters used in the simulation

Parameters	*Symbols*	*Value/range*	*Unit*
Channel length before the valve	L_1	*5.5, 5 ,4, 3, 2 and 1*	*[mm]*
Valve length	L_2	*0.5, 1, 2, 3, 4 and 5*	*[mm]*
Channel width	W_0	*2*	*[mm]*
Channel length after the valve	L_3	*22-*L_2	*[mm]*
Paper strip thickness	t	*0.18*	*[mm]*
Surface tension	γ	*0.072*	*[N/m]*
Surface tension in valve	γ_{valve}	*0.072*	*[N/m]*
Contact angle	θ	*83*	*[deg]*
Contact angle in valve	θ_{valve}	*90, 83, 66*	*[deg]*
Pore radius	R_c	*11*	*[µm]*
Valve pore radius	$R_{c_{valve}}$	*11, 8, 5.5, 5, 4, 3.5 and 3*	*[µm]*
Pore size distribution index	*lp*	*2*	*1*
Porosity	ε	*0.69*	*1*
Valve porosity	ε_{valve}	*0.9, 0.69, 0.4, 0.2, 0.1, 0.01 and 0.001*	*1*
Air density	ρ_{air}	*1*	*[kg/m³]*
Liquid density	ρ_{liquid}	*996*	*[kg/m³]*
Air viscosity	μ_{air}	*1.76 e-5*	*[Pa*s]*
Liquid viscosity	μ_{liquid}	*0.86*	*[mPa*s]*

The entry capillary pressure (p_{ec}) was calculated by:

$$p_{ec} = \frac{2\gamma\cos\theta}{R_c} \quad \text{Equation S1}$$

Where γ was the surface tension, R_c was the pore radius and θ was the contact angle.

Since the liquid drop at the inlet, PDMS wall, and channel width may greatly affect the flow speed, a coefficient k (=0.041) was added to Equation S1 to correct the difference between the ideal situation and the real experiment:

$$p_{ec} = \frac{2k\gamma \cos\theta}{R_c} \qquad \text{Equation S2}$$

The capillary pressure (outlet boundary condition) was given by:

$$p_c = p_{ec} \frac{1}{(\overline{s_w})^{1/\lambda_p}} \qquad \text{Equation S3}$$

where p_{ec} is the entry capillary pressure, $\overline{s_w}$ is the mean volume fraction of the wetting phase and λ_p was the pore distribution index.

The relative permeabilities for the wetting and non-wetting phases, based on the Brooks and Corey model, were given by

$$\kappa_{rw} = (\overline{s_w})^{(3+\frac{2}{\lambda_p})} \qquad \text{Equation S4}$$

$$\kappa_{rn} = \bar{s_n}^2 (1 - (1 - \bar{s_n}))^{(1+\frac{2}{\lambda_p})} \qquad \text{Equation S5}$$

The permeability (κ) of paper and valve region was calculated by:

$$\kappa = \frac{\varepsilon {R_c}^2}{8} \qquad \text{Equation S6}$$

Where ε was the porosity and R_c was the pore radius.

1.2. Device fabrication

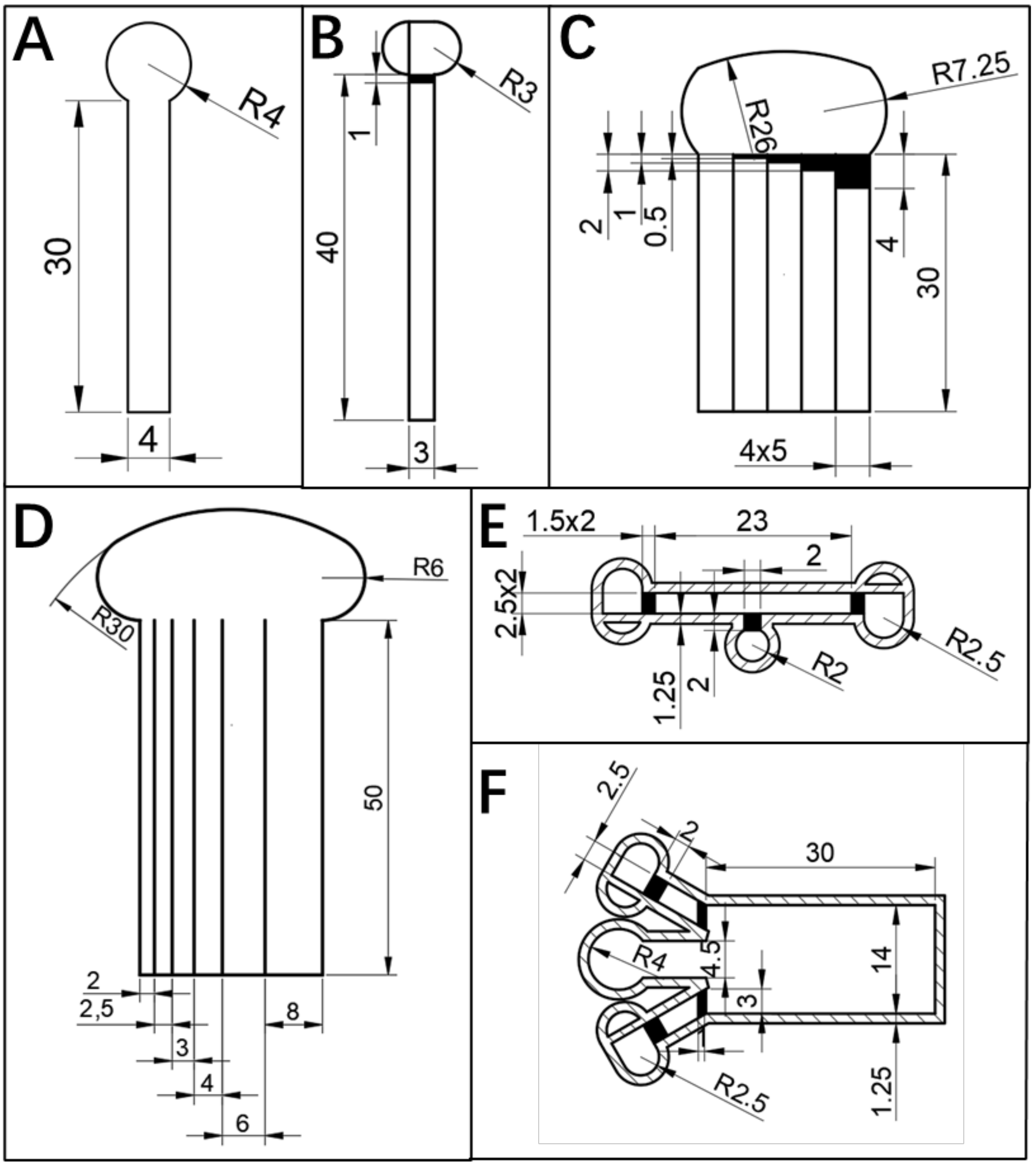

Figure S1 AutoCAD drawings for various chips. The μPADs for (A) flow study in PDMS surrounded channels, (B) glucose detection, (C) valve length study (with another similar design of valve length for 6, 8, 10, 12, 14), (D) channel width study, and (E) mixing and (F) parallel flow patterning after sequential loading. The unit of all dimensions is mm.

Figure S2 The automatic dispenser for PDMS wall printing.

1.3. Model validation

A mesh convergence test was performed and the grid of the valve area was encrypted to determine the size of mesh elements to acquire accurate results (Figure S3A). Afterward, a model with the same boundary conditions was created to evaluate the appropriateness of all critical simulation parameters (e.g. in Darcy's law) except for the properties of valves and fluids (Figure S3B).

Modified Lucas-Washburn equation[1] gave the analytical expression of the length of the liquid absorbed by the vertical paper strip:

$$L = \sqrt{\frac{k\gamma R_c t \cos\theta}{2\mu}} \quad \text{Equation S7}$$

Where L was the height of the liquid front, γ was the surface tension, R_c was the pore radius, θ was the contact angle, μ was the dynamic viscosity of water, and k (=0.041) was the correction coefficient.

The simulation results were compared with the data from both experiments and modified the Lucas-Washburn equation. The error was found less than 4.6% (Figure S3C).

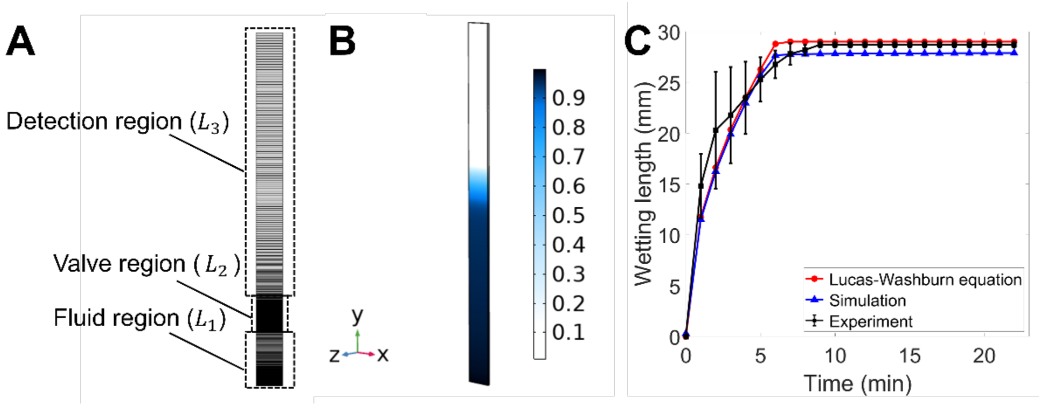

Figure S3 The model and validation results. (A) The 2D model and mesh created for the numerical study. The chip had three parts: a fluid region, a valve region, and a detection region. (B) Water saturation (3D) in the paper strip after 2 minutes. (C) The wetting length acquired from experiments, Lucas-Washburn equation, and simulation modified with a constant *k*.

1.4. Characterization of the wax valve

Table S3 Parameters of time-delay experiments.

Experiments	Surfactant concentration	Diffusion distance	Loading volume	Surfactant type
Diffusion distance (mm)	1	1-8	1	1
Surfactant type	Triton X-100			Tween 20
Surfactant concentration (%, v/v)	30			
Surfactant volume (μL)	0.6-2.2	2.2	2.2	0.4-2.2
Loading liquid	DI water			
Loading volume (μL)	30	60	10-30	30

3. Results

2.1 The numerical study of the flow delay mechanism

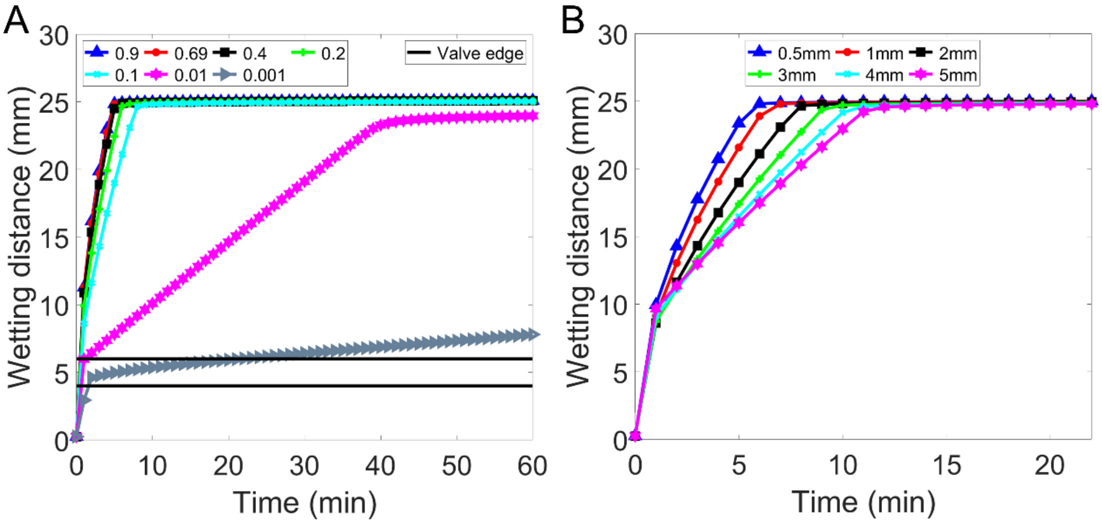

Figure S4 The numerical study of water flow in paper with valves. The wetting length when (A) the porosity and (B) the valve length varied.

2.2 Characterization of the wax valve

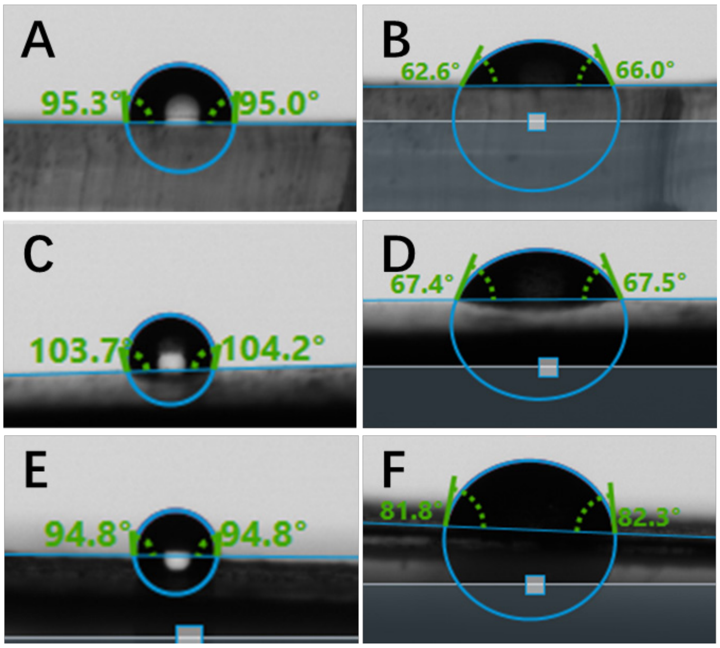

Figure S5 The photos for contact angle measurement. The photos of (A) water and (B) surfactant solution on the PDMS surface. The photos of (C) water and (D) surfactant solution on solid wax ink surface. The photos of (E) water and (F) surfactant solution on wax printed filter paper. All surfactant solution is 1.5% (v/v) Triton X-100 in DI water.

Table S4 The measured contact angle.

Liquid	Surfactant solution			Water		
Substrate	PDMS	Wax	Wax-printed paper	PDMS	Wax	Wax-printed paper
Contact angle	66.8°	66.0°	81.5°	95.9°	103.9°	94.9°
Standard deviation	5.0°	3.2°	2.0°	1.4°	0.7°	2.2°

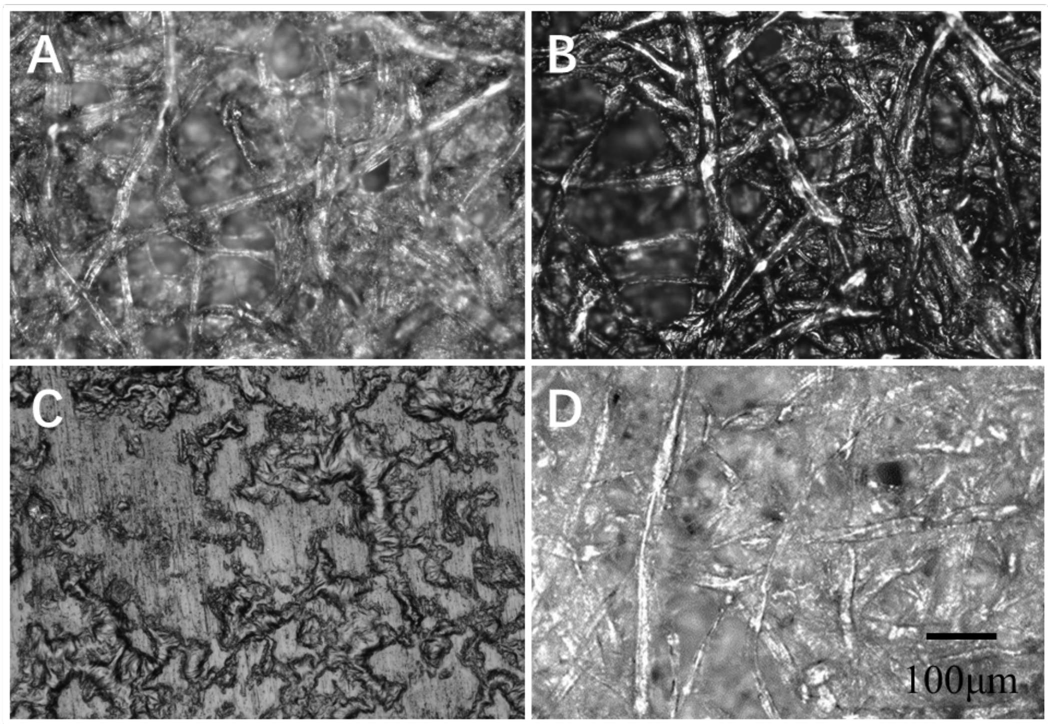

Figure S6 Micro-optical photos of the filter paper. The filter paper printed (A) one time and (B) three times on each side. (C) The filter paper with six-time wax printing and heated in a vacuum oven. (D) The raw filter paper

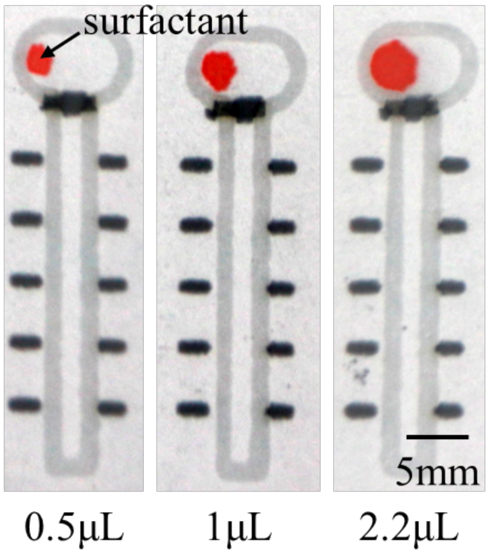

Figure S7 The photos of devices without the PDMS barrier for the surfactant loading zone. Red dye was added to the surfactant to demonstrate the spreading area of different surfactant volume.

2.3 High-sensitivity glucose detection

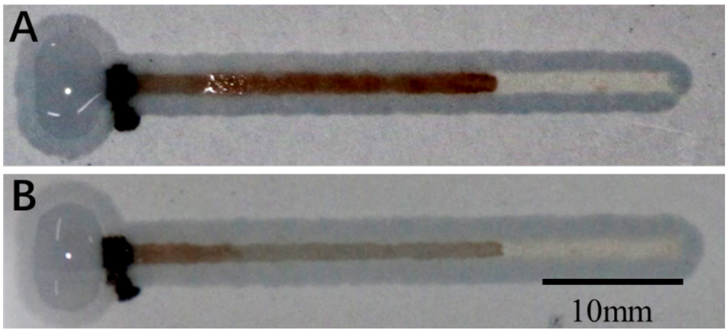

Figure S8 The photos of μPADs for glucose detection. (A) The μPAD detecting 200 mg/dL glucose solution 10 minutes after valve opening. The color length was equal to the wetting length. (B) The μPAD detecting 20 mg/dL glucose solution 10 minutes after valve opening. The color length was shorter than the wetting length.

4. Supplementary videos

Supplementary video S1 The PDMS barrier printing process using a dispenser.

Supplementary video S2 Flow of red dye in PDMS channels of different widths.

Supplementary video S3 Flow of red dye with surfactant (1.5% v/v) in PDMS channels of different widths.

Supplementary video S4 Flow of red dye with surfactant (1.5% v/v) through wax valves of different lengths.

Supplementary video S5 Sequential loading process of green and red dye using time-delay valves.

Supplementary video S6 Parallel flow patterning of blue, yellow, and red dye using time-delay valves.

Reference

1. E. W. Washburn, *Physical review*, 1921, **17**, 273.